Journal of Chromatography A, 659 (1994) 417–426
Elsevier Science B.V., Amsterdam

CHROM. 25 695

Computational simulation of migration and dispersion in free capillary zone electrophoresis

II. Results of simulation and comparison with measurements

J.C. Reijenga

Department of Chemical Engineering, Eindhoven University of Technology, P.O. Box 513, 5600 MB Eindhoven (Netherlands)

E. Kenndler*

Institute of Analytical Chemistry, University of Vienna, Währingerstrasse 38, A-1090 Vienna (Austria)

(First received June 24th, 1993; revised manuscript received September 10th, 1993)

ABSTRACT

The results of the simulation of electropherograms for CZE obtained by the instrumental simulator described in Part I are presented as functions of various experimental parameters. The electropherograms, demonstrating the effects of the injection zone length and sample composition on peak broadening, of the ζ potential on migration and efficiency, of minute changes in pH on the resolution, of the ionic strength of the buffer on the separation selectivity and of the co-ion of the background electrolyte on peak shape, are simulated within a few seconds. A comparison was made between simulated electropherograms and those obtained by measurements with real equipment.

INTRODUCTION

The theoretical background of the instrumental simulator introduced in Part I [1] was described there in detail. It provides in a fast way to simulate electropherograms as a function of a number of instrumental variables and physicochemical properties, based on two processes: migration and dispersion. For the calculation of the final result, depicted by the electropherogram, the appropriate expressions are used which take into account the analyte and the system features. Their consequences and limitations were discussed in detail in Part I.

It is the aim of this second part to demonstrate the performance of the simulation based on the plausibility of the resulting electropherograms, rather than to aspire to maximum agreement with experimental data. The latter will always be limited not only by the approximations of the theoretical model, but also by the quality of the input data necessary for the simulation (mainly pK values and absolute mobilities), which is often difficult to estimate.

In this paper, first the results are discussed when working parameters such as injection zone length, ζ potential and composition of the buffer are varied. The simulation illustrates that partially unexpected large effects on the electropherograms occur. The simulator is able to show, *e.g.*,

* Corresponding author.

SSDI 0021-9673(93)E1141-L

the significant influence of a likewise minute ζ potential (or electroosmotic mobility) on ion migration, a fact which is especially important when working with capillaries with a coated inner surface. Another example reflects the possible role of extremely small changes in the pH of the buffer, even in the range of a few hundredths of a unit. The normally underestimated role of the ionic strength on the separation selectivity, and possibly on the migration order of the separands, can also be demonstrated by simulation.

Second, a comparison is made of electropherograms measured with real equipment under given conditions with those resulting from the simulation. Some of these comparisons are carried out in pH ranges which are critical for the shape of the electropherograms. A comparison is finally made with two results published by Poppe [2], one obtained with another simulation algorithm, based on eigenvalues, and the other resulting from measurements.

EXPERIMENTAL

Chemicals

The chemicals used for the preparation of the standards and buffers and for the coating of the capillary were of highest available purity obtained from Merck (Darmstadt, Germany), EGA (Steinheim, Germany) and Fluka (Buchs, Switzerland). For the coating of the capillary, methylcellulose (Methocel MC, 3000–5000 mPa s; Fluka) was used. Water was doubly distilled from a quartz apparatus before use.

Apparatus

The electropherograms were measured with an instrument (P/ACE System 2000; Beckman, Palo Alto, CA, USA), which was equipped with a UV absorbance detector set at 214 nm. The system was controlled by a computer system with GOLD software (Beckman), which was also used for data acquisition.

The inner surface of the fused-silica capillary (269 mm overall length, 201 mm length to the detector, 75 μm I.D., 275 μm O.D.) (Scientific Glass Engineering, Ringwood, Australia) was coated according to a procedure described by Hjertén [3] in order to suppress electroosmosis for a number of experiments. The capillary was thermostated at 25.0°C.

The computer simulations were carried out as described in Part I [1].

RESULTS AND DISCUSSION

Variation of instrumental parameters

The results of the simulation will be discussed for the following examples: (i) the influence of the length of the injection zone on the peak width, with and without sample stacking; (ii) the influence of a very small ζ potential (or electroosmotic mobility) on migration times (and efficiency); (iii) the influence of the pH of the buffer on the resolution; (iv) the effect of the ionic strength of the buffer on the selectivity; and (v) the influence of the co-ion mobility on the electromigration dispersion (concentration overload).

Influence of injection width and sample composition. The length of the injection zone can contribute significantly to the total peak width according to the additivity of the variances of the individual contributions to peak broadening [4]. This effect is visible especially when the dispersion due to the dynamic processes is very low, which is often the case when a high voltage is applied and when the analytes carry a high effective charge number. The influence of the large injection volume can be dominant also when stacking cannot be achieved owing to the composition of the sample. From Fig. 1, it can be seen that the increase in the length of the injection zone, caused by an increase in the sampling time from 2 to 8 s (at a pressure of 5 mbar), can lead to a drastic decrease in resolution, especially when the sample is dissolved in buffer. The length of the injection zone increases from 0.71 mm at 2 s to 2.8 mm at 8 s under the given conditions, at an effective length of the capillary of 200 mm. The two last appearing peaks (4 and 5 in Fig. 1), which are separated with baseline resolution at an injection time of 2 s, show a highly reduced resolution at the longer sampling interval. This is caused by the fact that the plate height contribution due to the long injection zone, H_{inj} (about 4 μm at an

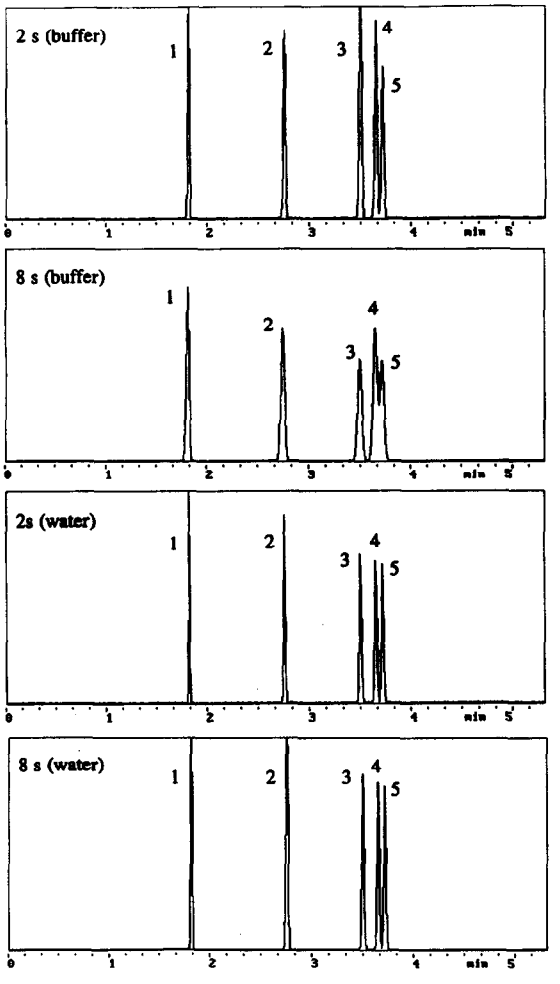

Fig. 1. Simulated electropherograms demonstrating peak broadening due to extra-column effects (length of injection zone) and sample stacking. Capillary: overall length 250 mm (effective length from injector to detector 200 mm) × 75 μm I.D. × 175 μm O.D.; voltage, −10 000 V; ζ potential, −3 mV (open mode); cooling temperature, 25.0°C. Buffer: pH 6.00; ionic strength, 0.010 mol/l; buffer ion mobilities, $-24.0 \cdot 10^{-9}$ and $+25.0 \cdot 10^{-9}$ $m^2/V \cdot s$. Injection: hydrodynamic, varying time: 2 or 8 s; 5.0 mbar; from water or buffer. Detection: "universal"; attenuation, 3 (2 s) or 10 (8 s); slit width, 200 μm; time constant, 0.10 s. Sample: 1 = 1,3-benzenedicarboxylate; 2 = 2,6-dinitrophenolate; 3 = 2,3-dimethoxybenzoate; 4 = 3,4-dimethoxybenzoate; 5 = 2,4-dimethoxybenzoate. Concentration: 100 μmol/l each.

8-s sampling time), given by eqn. 17 in Part I, predominates the total plate height, H, given by eqn. 37 in Part I, which is about 6 μm for these components.

If the sample is dissolved in pure water, and not in buffer (or in a solution with a similarly high conductivity), sample stacking occurs, and a concentrating and enrichment step leads to a shorter, sharper injection zone. In the case under consideration a stacking factor of about 10 is achieved. This effect can clearly be seen by comparing the corresponding electropherograms in Fig. 1. The two last peaks are still separated with baseline resolution even at an injection time of 8 s, caused by the improvement in the efficiency due to stacking: the plate height at 8 s is about 1.6 μm for these components, which is nearly the same as for a 2-s sampling time from water, and is even slightly better than at a 2-s injection time from buffer, where about 1.9 μm is observed. The large enhancement of efficiency by the stacking process can be seen from the plate height compared with that reached for an 8-s injection time from buffer, which is 6 μm and more, as mentioned above.

Influence of small ζ potentials on migration and efficiency. The problem of the variation of the ζ potential within one capillary under experimental conditions in practice was discussed in Part I. The simulation is nevertheless able to demonstrate how both the migration time and the efficiency are influenced by even very low ζ potentials. This result is important for systems where the electroosmotic migration is supressed but not eliminated entirely, which can be the case when working with coated columns. In these cases the electroosmotic velocity is difficult to determine by measurements with electrically neutral flow markers. The migration velocity of such a marker at, *e.g.*, 7 kV voltage across a 27 cm long capillary is only 0.02 mm/s for a ζ potential of −1 mV. This is the case when the initial ζ potential (about −120 mV for fused silica at high pH) is suppressed by more than 99%. The detector, placed, *e.g.*, at a 20-cm distance from the injector, is reached after 2.8 h, which is normally too long to be measured. Even for a five times higher ζ potential an electroosmotic velocity of 0.09 mm/s leads to a migration time of the neutral marker of 37 min in such a short capillary, so that the occurrence of an electroosmotic flow is thus often not noticed.

In the case under discussion, the separation of

anions is simulated in a fused-silica capillary with very reduced electroosmosis, reflecting the conditions in coated capillaries with a low residual ζ potential. The voltage is applied such that the separands are migrating to the anode (the electroosmotic flow is directed to the cathode, the reverse direction of the anion movement). From Table I it can be seen that this small ζ potential can, however, significantly influence the migration times of the separands in an open system as given by eqn. 12 in Part I (in closed systems no contribution to ion migration due to electroosmosis is assumed; in such cases only the efficiency is decreased).

Even such a small ζ potential as -1 mV influences the migration times considerably, especially for anions with low mobility. It can be seen that the migration times show a bias of as much as about 2% at this ζ potential in an open capillary, when compared with a closed capillary system. The deviation of the migration time at -5 mV is larger than 10% compared with the case without electroosmosis. This deviation is much larger than that which can be expected in capillaries with excluded electroosmosis. Although the resolution of the separands will not change dramatically under the given conditions (the electroosmotic mobility is small relative to the effective mobilities of the separands), it is seen that the determination of mobilities from the migration times in coated capillaries must be critically proved in order to obtain accurate values. One possibility is to control the extent of electroosmosis by calibration with a reference ion of known effective (or actual) mobility at the ionic strength of the system, or to work in a closed system [5].

For the case under discussion, the plate numbers of the anions decrease with increasing electroosmotic velocity, which is in accordance with the fact that the plate height (due to diffusional, thermal and electromigration dispersion) is directly proportional to the electromigration factor $f_{em} = u_{eff}/(u_{eff} + u_{eo})$, where u_{eff} and u_{eo} are the effective and the electroosmotic mobilities, respectively (see eqns. 23, 27, 31, 36 and 37 in Part I and ref. 6). As u_{eff} and u_{eo} have opposite signs in the example given, the denominator decreases as long as $|u_{eff}| > |u_{eo}|$, and thus H increases. For cations the reverse case is valid, leading always to an increase in the plate number with increasing electroosmotic mobility (but, however, to a decrease in resolution, as discussed in a previous paper [6]).

In the example simulated, the plate count N decreases by only 10%. Anyway, the simulation

TABLE I

INFLUENCE OF LOW ζ POTENTIALS ON MIGRATION TIMES

The migration times were calculated for the following conditions: effective capillary length, 20 cm (27 cm total), closed and open modes; voltage, -7000 V; ζ potential, -1 or -5 mV; buffer, pH 4.50, ionic strength 0.010 mol/l.

Separand	Migration time (min)		
	-1 mV[a] (closed)[b]	-1 mV[a] (open)[c]	-5 mV[a] (open)[d]
1,3,5-Benzenetricarboxylate	2.88	2.92	3.12
1,2,4-Benzenetricarboxylate	2.96	3.01	3.22
1,4-Benzenedicarboxylate	3.45	3.52	3.81
1,3-Benzenedicarboxylate	3.62	3.70	4.02
1,2-Benzenedicarboxylate	4.04	4.13	4.54

[a] ζ potential.
[b] $u_{eo} = 0$.
[c] $u_{eo} = 0.8 \cdot 10^{-9}$ m^2/V·s.
[d] $u_{eo} = 4.0 \cdot 10^{-9}$ m^2/V·s.

shows that the occurrence of a residual ζ potential can significantly affect the electrophoretic behaviour of the analytes. As the occurrence of such low ζ potentials can hardly be controlled in normal equipment, it can be one of the sources of the low quality of migration data thus obtained.

Influence of pH on resolution. The pH of the buffering background electrolyte influences both parameters which are decisive for the resolution, namely the selectivity and the efficiency. The former is determined by the effective mobilities of the separands and the latter by their effective charge numbers [6,7].

It was described in previous papers [8,9] that within a critical region even minute variations of the pH, namely in the range of a few hundredths of a unit, can drastically affect the resolution of two components. It was described, *e.g.*, in ref. 8 that certain separands co-migrated at pH 4.40 but were baseline resolved at pH 4.43. In this work a similar case was chosen for other pairs of ions in such a sensitive pH range. The result of this simulation is shown in Fig. 2. It can be observed that for two components (2 and 3) that form a single peak at pH 4.68, an increase of only 0.05 pH unit leads to baseline resolution.

Influence of ionic strength on separation selectivity. The migration behaviour of the separands is influenced by the concentration dependence of their actual mobilities as given by eqn. 8 in Part I (the effect of the ionic strength of the pK is neglected in this instance). Ions with equal charge are influenced to the same extent, so that no selectivity effects can be expected on varying the ion strength. In contrast, in mixtures of ions with different charge, the selectivity can be affected by the concentration of the buffer, and in some instances even the migration sequence can be reversed. This is demonstrated in Fig. 3, showing the electropherograms of the anions of two dibasic and one tribasic acid at different ionic strengths, I, of the buffer. The sequence is 1,4-dicarboxybenzoate, 1,2,3-tricarboxybenzoate and 1,3-dicarboxybenzoate at I = 0.010 mol/l, where the first two components are in fact unresolved. Although a narrow interval of the ionic strength was chosen, much less than one decade, the effect on the selectivity and even

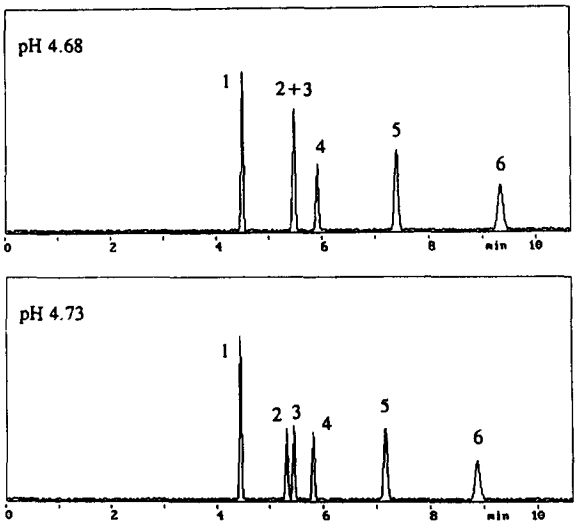

Fig. 2. Simulation of the effect of extremely small changes (a few hundredths of a pH unit) of the pH of the buffer on the resolution. Capillary: overall length 269 mm (effective length 202 mm) × 75 μm I.D. × 175 μm O.D.; voltage, −7000 V; ζ potential, −1 mV (open mode); cooling temperature, 25.0°C. Buffer: pH 4.68 (top) or 4.73 (bottom); ionic strength, 0.010 mol/l; buffer ion mobilities, $-24.0 \cdot 10^{-9}$ and $+25.0 \cdot 10^{-9}$ $m^2/V \cdot s$. Injection: hydrodynamic, 2 s, 5.0 mbar; from buffer. Detection: "universal"; attenuation, 3; slit width, 100 μm; time constant, 0.10 s. Sample: 1 = 2,6-dinitrophenolate; 2 = benzoate; 3 = 2,3-dimethoxybenzoate; 4 = 3,5-dimethoxybenzoate; 5 = 3,4-dimethoxybenzoate; 6 = 2,4-dimethoxybenzoate. Concentration: 100 μmol/l each.

on the migration order of the three separands is striking.

An increase in I leads to a decrease in the mobilities of all three separands (hence the migration times increase), but that of the trivalent analyte is most pronounced. 1,2,3-Tricarboxybenzoate migrates between the two divalent ions at I = 0.030 mol/l, where baseline separation of all three ions is obtained. The specific decrease in the actual mobility of the trivalent ion at higher ionic strength (0.045 mol/l) leads to a further increase in its migration time relative to the other two separands, and 1,3-di- and 1,2,3-tricarboxybenzoate now co-migrate.

Influence of the mobility of the co-ion of the background electrolyte on peak dispersion. As an example of the influence of the co-ion mobility on plate count and peak shape (eqs. 35 and 36 in Part I), the simulation was carried out for four

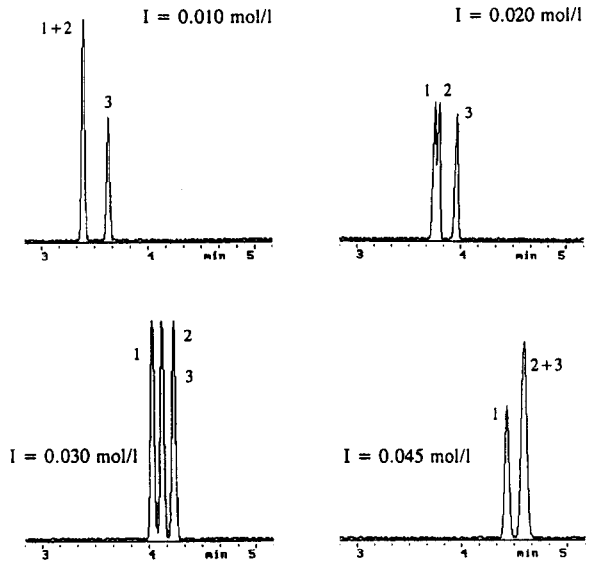

Fig. 3. Simulated electropherograms demonstrating the effect of the ionic strength, I, on the electrophoretic selectivity and resolution of multivalent anions with different charge at constant pH. Capillary: as in Fig. 2; voltage, −10 000 V; ζ potential, −20 mV (open mode); cooling temperature, 25.0°C. Buffer: pH 4.70; ionic strength, I, varying between 0.010 and 0.045 mol/l; buffer ion mobilities, $-30.0 \cdot 10^{-9}$ and $+25.0 \cdot 10^{-9}$ $m^2/V \cdot s$. Injection and detection: as in Fig. 2. Sample: 1 = 1,4-benzenedicarboxylate; 2 = 1,2,3-benzenetricarboxylate; 3 = 1,3-benzenedicarboxylate. Concentration: 100 μmol/l each.

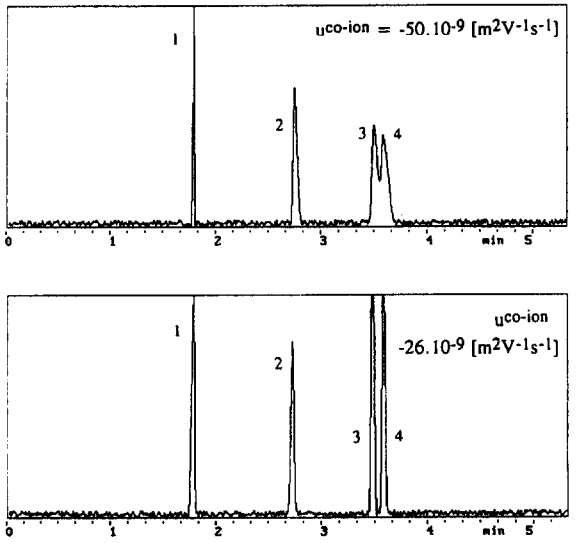

Fig. 4. Simulation of concentration overload (electromigration dispersion) for anions at different mobility of the co-ion of the buffering electrolyte. The simulation as made with a buffer at pH 7.00, ionic strength 0.010 mol/l, and a counter ion mobility of $+25 \cdot 10^{-9}$ $m^2/V \cdot s$. The effective mobility of the co-anion is $-50.0 \cdot 10^{-9}$ $m^2/V \cdot s$ (top) and $-26.0 \cdot 10^{-9}$ $m^2/V \cdot s$ (bottom). Voltage, −10 000 V; capillary dimensions as in Fig. 1; ζ potential, −3 mV, (open mode); injection, 2 s (5 mbar) from buffer. Detection: "universal"; slit width, 100 μm; time constant, 0.05 s; attenuation, 10. Sample: 1 = 1,3-benzenedicarboxylate; 2 = 2,6-dinitrophenolate; 3 = 2,3-dimethoxybenzoate; 4 = 3,4-dimethoxybenzoate. Sample concentrations: 500 μmol/l each. For effective mobilities of sample components at the given pH, see Table II.

separands with different effective mobilities, given in Fig. 4 and Table II. In this example the co-ion mobility of the background electrolyte is adjusted to the mobility of the first- or the last-migrating component. These mobilities are $-49.5 \cdot 10^{-9}$ and $-25.7 \cdot 10^{-9}$ $m^2/V \cdot s$, respectively. It can be observed that in both instances the peaks of the components with a mobility that differs from that of the co-ion show partially strong asymmetry, which is expressed by the skew (a symmetrical peak has a skew of zero). In the first example these peaks are triangular-shaped with tailing (the skew has a positive sign) and in the second instance with leading (negative sign of the skew).

The plate number is low in the second example for the fastest ion, namely only about 16 000, despite to the fact that this ion has an effective charge of 2. The last migrating ion has about 100 000 plates under the given conditions, about six times more than for the first component, although the latter has an effective charge number which is only one half of that of the former. The reason for this behaviour can be derived from the values of the individual contributions of the peak-broadening effects. The plate-height contributions due to Joule heating, electroosmosis, detector slit width and time constant are negligible (each less than 0.1 μm), and that from injection is also relatively low (0.4 μm). In contrast, those caused by diffusion and concentration overload, given in Table II, are significant. For component 1 the plate-height contribution due to electromigration dispersion, H_{conc}, (11.8 μm) exceeds that from diffusion (0.7 μm) by a factor of 17 when the co-ion mobility is

TABLE II

EFFECT OF CO-ION MOBILITY OF THE BACKGROUND ELECTROLYTE ON THE TWO MAIN CONTRIBUTIONS TO THE TOTAL PLATE HEIGHT, H, DUE TO DIFFUSION (H_{dif}) AND CONCENTRATION OVERLOAD (H_{conc}), AND TO PEAK SYMMETRY FOR FOUR SEPARANDS (1–4) WITH DIFFERENT EFFECTIVE MOBILITIES

H is given in μm. Peak asymmetry is expressed by the skew. The effective mobilities of the separands under the given conditions are (1) $-49.5 \cdot 10^{-9}$, (2) $-33.0 \cdot 10^{-9}$, (3) $-26.4 \cdot 10^{-9}$ and (4) $-25.7 \cdot 10^{-9}$ m^2/V·s. For details (*e.g.*, on percentage triangle) see Part I.

Parameter	Co-ion mobility							
	$-50 \cdot 10^{-9}$ m^2/V·s				$-26 \cdot 10^{-9}$ m^2/V·s			
	1[a]	2[a]	3[a]	4[a]	1[a]	2[a]	3[a]	4[a]
H_{dif}	0.67	1.37	1.40	1.40	0.67	1.37	1.40	1.40
H_{conc}	0.17	8.02	13.5	14.2	11.8	4.24	0.26	0.19
H_{tot}	1.51	9.93	15.4	16.1	13.1	6.09	2.13	2.06
Skew	+0.53	+1.51	+1.51	+1.51	−1.50	−1.50	−0.57	+0.44
% triangle	11	81	87	88	91	70	12	9

[a] Numbering of separands as in Fig. 4.

$-26 \cdot 10^{-9}$ m^2/V·s, and is the main source of peak broadening for this component. This concentration overload causes the triangular shape of the peaks of the fastest components, indicated by a value of −1.5 for the skew. The last-migrating component, on the other hand, to which the mobility of the co-ion is adjusted, shows a negligible contribution due to concentration overload (about 0.2 μm), so that the total plate height of 2.1 μm is in fact predominantly caused by diffusion. The peak is nearly symmetrical: the skew is only 0.4.

When identical electrophoretic conditions are applied, but the co-ion mobility is adjusted to the effective mobility of the fastest ion ($-49.5 \cdot 10^{-9}$ m^2/V·s), this component now exhibits the highest peak symmetry and the lowest plate height. The diffusional dispersion determines the total plate height for this peak 1, in contrast to peak 4, where the concentration overload dominates.

Comparison of simulated with measured electropherograms

A number of examples are given for a comparison of simulated electropherograms with those obtained by experiment. The latter were measured in the context of other investigations, and were not prepared specially to fit to the simulation. They were all measured using a UV absorbance detector at 214 nm. They were compared with the simulated electropherograms obtained using either a "universal" detection mode or by conductivity detection.

In Fig. 5 the electropherogram of three separands (dimethoxybenzoic acids) is shown, which was measured for the investigation of the adjustment of resolution and analysis time by the buffering pH [8]. It can be seen that the electropherogram obtained by simulations is nearly identical with the experimental trace. The small deviations in the migration times are due to the systematic error which is made in the calculation of the mobilities used for simulation, and which is nearly inevitable considering the various steps of approximation involved here: from measured migration times the actual mobilities are calculated for the ionic strength of the experimental conditions, from those the values of the absolute mobilities are approximated, from which finally the actual and the effective mobilities for the ionic strength conditions of the simulation are

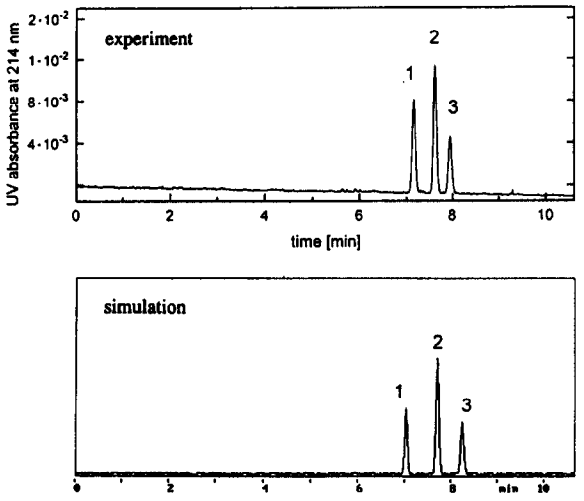

Fig. 5. Comparison of a measured electropherogram of three benzoic acids with the simulation under comparable conditions. Experimental conditions (top): coated capillary, overall length 269 mm (effective length from injector to detector 201 mm) × 75 μm I.D. × 275 μm O.D.; voltage, −5000 V; temperature, 25.0°C; buffer, pH 5.33 (acetic acid–sodium acetate, *ca.* 0.01 mol/l); injection, pneumatic for 1 s. Simulation conditions (bottom): ζ potential −1 mV (open mode); ionic strength, 0.010 mol/l; buffer ion mobilities, $-35.0 \cdot 10^{-9}$ and $+25.0 \cdot 10^{-9}$ $m^2/V \cdot s$; injection, hydrodynamic, 2 s, 5.0 mbar; from water. Detection: "universal"; attenuation, 1; slit width, 100 μm; time constant, 0.010 s. Sample: 1 = 2,3-dimethoxybenzoate (50 μmol/l); 2 = 3,4-dimethoxybenzoate (100 μmol/l); 3 = 2,4-dimethoxybenzoate (50 μmol/l).

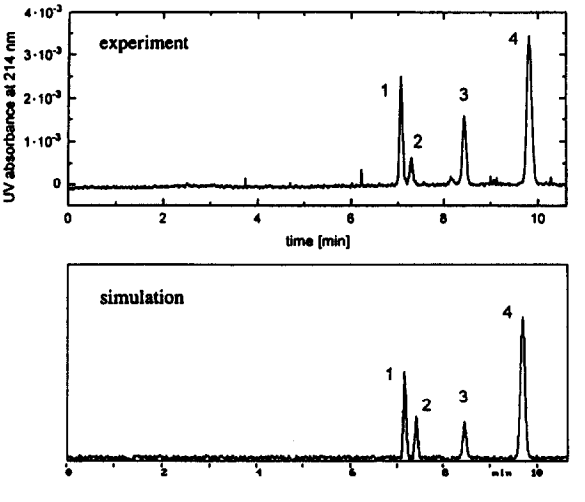

Fig. 6. Comparison of simulated and measured electropherograms of monobasic acids at a pH critical for the resolution of components 1 and 2. Experimental conditions (top): capillary, voltage, cooling temperature, injection and detection as in Fig. 5; buffer, pH 4.99 (acetic acid–sodium acetate, *ca.* 0.01 mol/l). Simulation (bottom): pH 4.99; ionic strength, 0.010 mol/l; buffer ion mobilities, $-24.0 \cdot 10^{-9}$ and $+25.0 \cdot 10^{-9}$ $m^2/V \cdot s$; injection, hydrodynamic, 2 s, 5.0 mbar; from water. Detection: "universal"; attenuation, 3; slit width, 100 μm; time constant, 0.020 s. Sample: 1 = 2,3-dimethoxybenzoate (200 μmol/l); 2 = 3,5-dimethoxybenzoate (100 μmol/l); 3 = 3,4-dimethoxybenzoate (100 μmol/l); 4 = 2,4-dimethoxybenzoate (500 μmol/l).

derived. Based on these approximations, it is found that the simulated migration times agree fairly well with those on the measured electropherogram, namely within 1–3%.

A more complex case is shown in Fig. 6, where the pH is in the narrow range critical for the separation of two of the components under consideration. Experimentally the pH was adjusted to that unique value at which baseline separation of all components was predicted within the shortest time of analysis, according to a theoretical approach presented in previous papers [8,9]. In the case under consideration, the given resolution is established for the first pair of components exactly at pH 4.99. In fact, at this pH the result of the calculation of the resolution is in agreement with the experimental finding. The simulation for various conditions is striking: the same resolution results at exactly that pH as in the experiment. It should be pointed out that this good result is obtained despite the fact that the effective mobilities, calculated from the absolute mobilities (at infinite dilution), were extrapolated to the ionic strength conditions with a fairly rough approximation, as given by eqn. 8 in Part I, which is currently under investigation [10].

Another complex example is demonstrated by six other separands, where the pH range for the migration order as for the resolution of three of the separands is also critical [9]. At pH 5.03 the separands 1,4-di-, 1,2,3-tri- and 1,3-dicarboxybenzoate migrate closely in the sequence given above, as can be seen from the measured electropherogram (Fig. 7, top), and form a triplet of nearly unresolved peaks. The simulation is in agreement in this instance also (Fig. 7, bottom), although the larger number of actual

mobilities and pK values necessary for the simulation can be potential sources of deviations: co-migration is simulated in addition to the correct sequence.

Finally, the result of the simulation including electroosmotic flow is compared with two electropherograms published by Poppe [2], one obtained experimentally using indirect UV detection and the other calculated by an algorithm based on eigenvectors and eigenvalues, as shown in Fig. 8. It demonstrates the separation of seven amino acids at pH 11.0. Our simulation is in agreement with both of Poppe's results. Not only is the migration sequence identical, but also the peak distortion (especially the triangulation due to concentration overload) is clearly simulated.

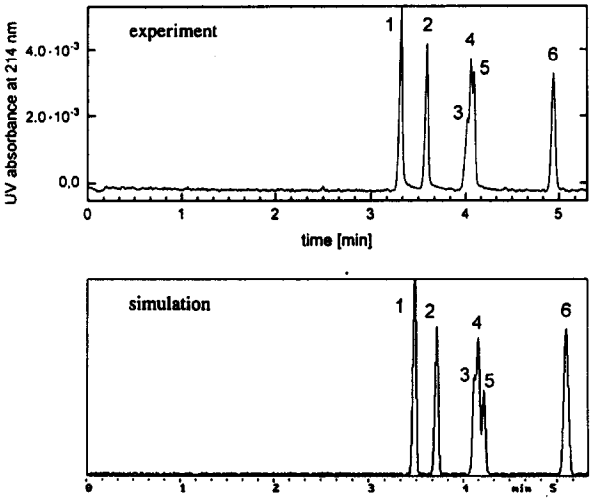

Fig. 7. Comparison of simulated and measured electropherograms of di- and tribasic benzoic acids at pH 5.03. Experimental conditions (top): capillary, voltage, cooling temperature, injection and detection as in Fig. 5; buffer, acetic acid–sodium acetate, *ca.* 0.01 mol/l. Simulation (bottom): ζ potential, −1 mV (open mode); buffer ionic strength, 0.012 mol/l; buffer ion mobilities, $-24.0 \cdot 10^{-9}$ and $+25.0 \cdot 10^{-9}$ m^2/V·s; injection, hydrodynamic, 2 s, 5.0 mbar; from buffer. Detection: "universal"; attenuation, 3; slit width, 100 μm; time constant, 0.010 s. Sample: 1 = 1,3,5-benzenetricarboxylate (200 μmol/l); 2 = 1,2,4-benzenetricarboxylate (200 μmol/l); 3 = 1,4-benzenedicarboxylate (100 μmol/l); 4 = 1,2,3-benzenetricarboxylate (200 μmol/l); 5 = 1,3-benzenedicarboxylate (100 μmol/l); 6 = 1,2-benzenedicarboxylate (200 μmol/l).

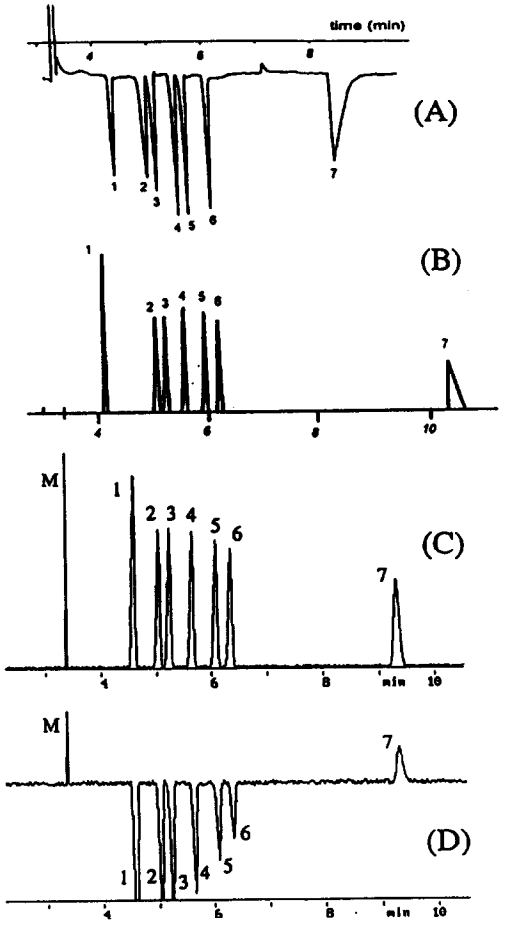

Fig. 8. Comparison of a measured electropherogram of amphoteric analytes (amino acids), including electroosmotic flow, with the result of a simulation based on an eigenvector approach, and with the instrumental simulator. Capillary: overall length 59 cm (effective length 36 cm) × 7.5 μm I.D.; voltage, +15 000 V; buffer, pH 11.0, concentration 0.01 mol/l. Analytes: 1 = proline; 2 = leucine; 3 = valine; 4 = alanine; 5 = serine; 6 = glycine; 7 = glutamic acid; M = neutral EOF marker. (A) Experimental result obtained by indirect UV detection using sodium salicylate as background electrolyte. Injection by electromigration at 6000 V for 5 s; $u_{eo} = 70 \cdot 10^{-9}$ m^2/V·s. Analyte concentrations: 0.001 mol/l each, dissolved in background electrolyte. From ref. 2. (B) Simulated electropherogram obtained by the eigenvector approach for the same conditions as in (A). From ref. 2. (C) Electropherogram obtained by the instrumental simulator for conditions as in (A). For the buffer ion mobilities the values taken were $-40 \cdot 10^{-9}$ and $+51 \cdot 10^{-9}$ m^2/V·s. Injection: 20 s from water (5.0 mbar). Detection: "universal"; attenuation, 30; slit width, 20 μm; time constant, 0.2 s. Analyte concentration: 0.0005 mol/l each. (D) Electropherogram obtained with the instrumental simulator in the conductivity detection mode. Conditions as in (C).

CONCLUSIONS

The examples given indicate that the theoretical model with its limitations and assumptions, as described in Part I, yields sufficiently realistic electropherograms to illustrate the integrated effect of almost all factors of importance in capillary zone electrophoresis. This enables our simulator to obtain a large number of results on the influence of many parameters on the electropherograms in a similarly short time, and thus offers great flexibility compared with other simulation systems, especially for demonstration and training purposes. This is a clear advantage over other algorithms, for which the calculations take minutes or even hours (possibly with greater accuracy of the prediction). From all the comparisons with experimental results it can be concluded that the simulator introduced here allows the depiction of the final electropherogram with good (although not always exact) agreement.

ACKNOWLEDGEMENT

The authors acknowledge the technical assistance of W. Friedl (Institute for Analytical Chemistry, University of Vienna, Vienna, Austria).

REFERENCES

1 J.C. Reijenga and E. Kenndler, *J. Chromatogr.*, 659 (1994) 403.
2 H. Poppe, *Anal. Chem.*, 64 (1992) 1908.
3 S. Hjertén, *Chem. Rev.*, 9 (1967) 122.
4 J. Sternberg, *Adv. Chromatogr.*, 2 (1966) 205–270.
5 Th.P.E.M. Verheggen and F.M. Everaerts, *J. Chromatogr.*, 638 (1993) 147.
6 C. Schwer and E. Kenndler, *Chromatographia*, 33 (1992) 331.
7 E. Kenndler and C. Schwer, *Anal. Chem.*, 63 (1991) 2499.
8 E. Kenndler and W. Friedl, *J. Chromatogr.*, 608 (1992) 161.
9 W. Friedl and E. Kenndler. *Anal. Chem.*, 65 (1993) 2003.
10 J.C. Reijenga, in preparation.